A novel carcinogenic PI3Kα mutation suggesting the role of helical domain in transmitting nSH2 regulatory signals to kinase domain

Safoura Ghalamkari
Isfahan University of Medical Sciences
Shahryar Alavi
University of Isfahan
Hamidreza Mianesaz
Isfahan University of Medical Sciences
Farinaz Khosravian
Isfahan University of Medical Sciences
Amir Bahreini
University of Pittsburgh
Mansoor Salehi (m_salehi@med.mui.ac.ir)
Isfahan University of Medical Sciences https://orcid.org/0000-0002-6565-0907

Research article

Keywords: Breast cancer, PIK3CA, novel mutation, MD simulation

Posted Date: February 13th, 2020

DOI: https://doi.org/10.21203/rs.2.12981/v3

Version of Record: A version of this preprint was published on March 15th, 2021. See the published version at https://doi.org/10.1016/j.lfs.2020.118759.

Abstract

Background Mutations in PIK3CA, which encodes p110 subunit of PI3K class IA enzyme, are highly frequent in breast cancer. Here, we aimed to probe mutations in exon 9 of PIK3CA and computationally simulate their function. Method PCR/HRM and PCR/sequencing were used for mutation detection in 40 breast cancer specimens. The identified mutations were queried via in silico algorithms to check the pathogenicity. The molecular dynamics (MD) simulations were utilized to assess the function of mutant proteins. Result Three samples were found to harbor at least one of the E542K, E545K and L551Q mutations of which L511Q has not been reported previously. All mutations were confirmed to be pathogenic and MD simulations revealed their impact on protein function and regulation. The novel L551Q mutant dynamics was similar to that of previously found carcinogenic mutants, E542K and E545K. A functional role for the helical domain was also suggested by which the inhibitory signal of p85α is conducted to kinase domain via helical domain. Helical domain mutations lead to impairment of kinase domain allosteric regulation. Interestingly, our results show that p110α substrate binding pocket of helical domain in mutants may have differential affinity for enzyme substrates, including anit-p110α drugs. Conclusion The novel p110α L551Q mutation could has carcinogenic feature similar to previously known mutations.

Background

Breast cancer is the second cause of death due to cancer in women worldwide (1). In 2018, breast cancer accounted for 30% of 1.7 million new cases of cancer that were reported in the US (2).

The Phosphatidylinositol 3 kinase (PI3K) pathway is one of the most important oncogenic signaling pathway in breast cancer tumorigenesis and the majority of breast tumors harbor at least one molecular defect in this pathway (3). PI3K pathway plays a key role in various cellular functions such as survival, proliferation, differentiation, and angiogenesis (4). Class IA PI3K enzymes are composed of one p110 catalytic subunit which binds to a p85 regulatory subunit, to form a functional enzyme. They are activated by receptor tyrosine kinases (RTKs) that remove inhibitory effect of p85 on p110 and therefore, PI3K becomes active. Among the members of class IA, p110α and p85α are expressed in most cells, encoded by *PIK3CA* and *PIK3R1* genes, respectively (5). Large genomic studies such as The Cancer Genome Atlas (TCGA) have revealed that *PIK3CA* is the most frequently mutated gene in breast cancer (6, 7). This data shows that ~40% of all breast tumors have at least one *PIK3CA* mutation that could be a representation of PI3K oncogenic pathway. The majority of hotspot gain-of-function *PIK3CA* mutations are clustered in exon 9 and 20 of the gene that correspond to the helical and kinase domains of p110α, respectively (8). Pathogenicity of E542K and E545K mutations located in exon 9 have been characterized by several studies suggesting that these mutations alter the interaction of helical domain and nSH2 and consequently, diminish the inhibitory effect of p85α on p110α (9). Another study (10) has shown that the mechanism of action of p110α mutations is not as simple as alterations in helical domain interactions with nSH2. In addition, a recent study (11) has suggested that p85α allosterically regulates p110α kinase

activity via helical domain. Generally this change makes hyper-activation of PI3Kα followed by activation of AKT leading to an uncontrolled cell division (9, 12).

Since breast cancer is a genetically complex and highly heterogeneous disease with diversity in therapeutic responses, our aim was to investigate the hotspot region in exon 9 of *PIK3CA* for pathogenic mutations using High Resolution Melting (HRM) followed by PCR+Sanger sequencing as a fast and cost-effective method for screening. Finally, we employed molecular dynamics simulation technique to study the potential function of the detected novel variants.

Methods

2.1 Tumor samples and DNA extraction

Tumor tissue was collected from 40 patients diagnosed with primary breast cancer ranging from 35 to 65 years of age. The study was approved by the ethics committee of Isfahan University of Medical Sciences and written informed consent was obtained from all the patients.

The tumor tissue was flash frozen in liquid nitrogen and DNA was extracted using Qiagen DNeasy Blood & Tissue kit (Qiagen, Germany).

2.2 PCR/HRM

PCR/HRM was used to identify samples with potential mutations on the hotspot region of exon 9 (from aa513 to aa554). The primer set that was used for amplifying the region of interest contained forward 5'TGACAAAGAACAGCTCAAAGCA-3' and reverse 5'-AGCACTTACCTGTGACTCCA-3 that produced a 96 bp amplicon. HRM analysis was performed using Corbett Research Rotor Gene-6000 (Qiagen-Germany) and the HRM Master Mix (Type-it HRM PCR Kit Qiagen-Germany). PCR was performed by incubating the reaction at 95°C for 5 minutes followed by 45 cycles of 95°C for 10 seconds, 64°C for 30 seconds and 72°C for 10 seconds. In the final step, HRM analysis was carried out from 70–85°C with ramping at 0.2°C/s. The PCR/HRM curve was analyzed via Q 5plex HRM software to compare unknown samples with wild type (WT) control.

2.3 Sanger sequencing

As a second approach to verify the detected hotspot mutations via PCR/HRM, DNA from all the HRM positive samples was amplified by 5'-CATCTGTGAATCCAGAGGGGA-3' as the forward and 5'-AGCACTTACCTGTGACTCCA-3' as the reverse primers producing an amplicon of 201bp. PCR products were purified using QIAquick PCR purification kit (Qiagen-Germany) and sequenced by ABI prism 3730 sequencer (Applied Biosystems, Waltham, MA, USA). The sequencing data was analyzed via Chromas version 2.33 software.2***In Silico*** **Prediction**

2.4 Algorithms

The pathogenicity of novel mutations in exon 9 of *PIK3CA* was investigated by several *in silico* tools that predict the deleterious effect of coding single nucleotide variants (SNVs). These include PolyPhen2 (13), SIFT (14), MutationTaster (15), PROVEAN (16), PhD-SNP (17), I-MutantDDG-Seq Suite (18) and Hope software (19). In addition several tumor mutation databases were searched for identified mutations including Catalog of Somatic Mutation in Cancer (20), My Cancer Genome (21) and TCGA (22).

2.5 Molecular Dynamics Simulations

PDB 4OVU (23) was used as the reference structure for molecular dynamics simulations. For simplicity, only helical and kinase domains of p110α (amino acids 519-1052) and nSH2 domain of p85α (327-430) were selected for later analysis. Four different systems were designed: WT, E542K, E545K, and L551Q. Structures of the mutated p110α were created by substituting the corresponding amino acids from WT.

Simulation boxes were made using Amber16/LEaP (24). Protein complexes were solvated into an octahedral TIP3P water model box with at least 15Å distance from box boundaries. Na^+ and Cl^- ions were added to neutralize and maintain 150 mM physiologic saline concentration. Each system contains about 113,000 atoms. Amber force field ff14SB was used in the simulations.

Simulations were run using GPU-accelerated version of Amber16. 4000 cycles of energy minimization were done, with the first 1500 cycles with restraints on *PIK3CA*. Systems were heated up to 310 K within 40 ps in 4 steps and simulations were continued to 100 nanoseconds (ns). SHAKE algorithm was used for hydrogen bonds and 2 femtoseconds time step was applied. Coordinates were captured every 10 ps.

Analyses were done using CPPTRAJ, and R package Bio3d 2.3 (25). Molecular visualizations were created using PyMOL (The PyMOL Molecular Graphics System, Version 1.9 Schrödinger, LLC.).

Results

3.1 Discovery of novel mutation in exon 9 of *PIK3CA*

Initial screening via PCR/HRM was performed on DNA extracted from 40 tumor samples and the HRM positive samples were subsequently investigated by Sanger sequencing for mutations on exon 9. Four tumors displayed an altered melting pattern in PCR/HRM of which three were confirmed to harbor at least one of the E542K, E545K or L551Q mutations. E542K and E545K variants were previously reported as pathogenic mutations in My Cancer Genome (21), cosmic (20) and TCGA (22), however, L551Q mutation did not exist in any of the cancer databases. Interestingly, the sample with L551Q variant had a pathogenic mutation, E542K, in hotspot region of exon 9 (Table 1). This prompted us to investigate the pathological effect of E542K, E545K, and the newly detected L551Q by further *in silico* studies.

3.2 p110α L551Q dynamics displays a carcinogenic activity

The impact of L551Q was first predicted to be disease causing using various variant annotation tools that is described in Table 2 in details. We then used molecular dynamics simulation to study the

structural effects of all mutations we found in p110α helical domain. Although the p110α-p85α is a large complex, the p110α kinase and p85α nSH2 domains are the main functional domains of the complex, with the p110α helical domain mediating their interactions (Figure 1). We restricted our simulation systems to these three domains that have the central role in PI3Kα activity to investigate how the kinase activity of p110α is regulated by p85α.

p110α helical domain directly interacts with the nSH2 domain of p85α but the function of this interaction has not been fully uncovered. Thus, first we compared the dynamics cross-correlation map (DCCM) of simulated systems to find out to what extent the motions of helical domain are correlated with nSH2 and kinase domains, and if helical domain mutations could affect this correlation (Figure 2). In WT, all of helical, kinase and nSH2 domains have a high intradomain correlation score. In addition, helical domain motions are highly correlated with nSH2 motions. N-terminal region of kinase domain is highly anti-correlated with helical and nSH2 domains whereas C-terminal region (encompassing the enzyme catalytic site) is highly correlated with helical and nSH2.

All of the mutant systems show a huge reduction in both intra and interdomain correlations (Figure 2). Surprisingly, the helical domain mutations have a greater impact on the kinase domain correlations. The pattern of DCCM from all mutants, including L551Q, are similar, in which helical domain and nSH2 show intradomain correlations, but their motions are no longer correlated with those of kinase domain, specifically in E545K. Additionally, the intradomain motions of kinase domain are disturbed, in particular in the C-terminal region.

To better visualize how helical domain mutations affect the overall motions of the p110α-p85α complex, we rendered dynamics of all systems along their first principal mode of motion (PC1) (Figure 2, tube structures). In WT, all of helical domain, kinase domain C-terminal region, and nSH2 domain residues move as an integrated unit. However, the N-terminal region of kinase domain is less dynamic and moves to an opposite direction, as shown as an anti-correlated moiety in the WT DCCM.

PC1 shows that helical domain mutations, including L551Q, have slowed down the dynamics of p110α-p85α complex, to the extent that kinase domain is almost static and does not respond to helical and nSH2 domains dynamics. In other words, there is no integrated motions of domains in the mutant complexes unlike what is seen in the WT. The helical and nSH2 domains move slowly towards the C-terminal region of kinase domain in E542K and E545K. Inversely, the helical domain slowly moves towards the N-terminal region of kinase domain in L551Q. The nSH2 domain residues in L551Q show erratic motions along their PC1.

Taken together, DCCM and PC analyses show that helical domain mutations extremely affect dynamics of p110α-p85α complex. In WT, motions of kinase domain are completely regulated by coordinated motions of helical and nSH2 domains. However, mutants have disrupted this dynamic regulation, turning kinase domain into a detached part which no longer moves with helical and nSH2 domains. Indeed, dynamic behavior of L551Q is compatible with that of E542K and E545K mutants. Thus, these results

strongly suggest that the novel p110α L551Q mutation could harbor carcinogenic features similar to previously known mutations.

3.3 nSH2 allosterically regulates p110α catalytic activity through helical domain

We then asked how a small change in helical domain can affect dynamics of kinase domain. To answer that, we utilized community network analysis to investigate the pathways that connect motions of kinase to helical and nSH2 domains. Edge betweenness measurements revealed that E542 mediates the communication between nSH2 and helical domains in WT. Then D538 in the helical domain, in vicinity of E542, interacts with N996 in the kinase domain, and directly spreads the nSH2 regulatory signal throughout the kinase domain (Figure 3A). So, these three residues (E542, D538, and N996) have a central role in conducting the regulatory signal from nSH2 domain to kinase domain.

As D538 is spatially oriented in the middle of the E542 and N996, changing the repulsive force of E542-D538 to an attractive one by E542K mutation influences the orientation of D538 relative to N996, and consequently disrupts the interaction between helical and kinase domains. Therefore, E542K mutant cannot conduct the nSH2 regulatory signal to kinase domain, but instead, diverts the signal to the helical domain, leading to the detachment of kinase domain from helical and nSH2 domains. On the other hand, E545K and L551Q mutations change helical-nSH2 and helical domain internal interaction respectively, both resulting in an impaired interaction of D538-N996.

For further confirmation of these results, we tried to find suboptimal pathways from nSH2 domain to three kinase domain residues including: K776 in the p-loop which identifies p110α substrate specificity, H917 in the catalytic loop which accommodate ATP and catalysis the enzymatic reaction, and K941 in the activation loop, which makes the initial interactions with substrates. In WT, signals from nSH2 domain allosterically regulate catalytic activity by two main pathways: one passes through kinase domain H12, and the other through helical domain (data not shown). In all mutants, these allosteric pathways become significantly longer (Figure 3B), because the nSH2 regulatory signal has been trapped in the helical domain.

Collectively, communication network analysis shows that the helical domain mutations disrupt the connection between helical and kinase domains, resulting in detachment of kinase domain from rest of the complex. Consequently, nSH2 signal is trapped in the helical domain since it cannot find its way towards kinase domain which makes it inaccessible to nSH2 domain in all three mutants.

3.4 P110α substrate affinity is different in each mutant

Some of the known mutants of p110α has been proved to result in resistance to anti-p110α drugs (26, 27). Thus, it is clinically important to find out whether breast cancer patients with the novel carcinogenic p110α L551Q mutation may be drug resistant. To this end, we investigated the flexibility and shape of the p110α substrate binding pocket (SBP) using pairwise root-mean-square deviation (RMSD) and radius of gyration (R_g) calculations, respectively. RMSD distribution plot (Figure 4) shows that the flexibility of the

SBP has been slightly reduced in all mutants, specifically in E545K, compared to WT. For an enzyme with various substrates, a more rigid SBP could result in higher affinity for a specific substrate. To further inspect this hypothesis about p110α catalytic site, we compared distributions of R_g of p110α SBP in all simulated systems (Figure 4B). R_g variation shows the major difference between E542K and E545K mutants, suggesting that the shape of apo-enzyme SBP differs among mutants ($p < 2.2e\text{-}16$).

Accordingly, geometric analysis suggests that all helical domain mutations result in a slightly rigid p110α SBP with different shapes. This proposes that a specific therapeutic compound may not have the same affinity for all p110α mutants. Further biophysical experiments are warranted to test this hypothesis.

Discussion

Our findings suggested that newly detected L551Q mutation may harbor carcinogenic features similarly to known mutations such as E545K and E542K located in p110α helical domain. Multiple *in silico* variant annotation tools showed that L551Q is likely to be disease causing. In addition, molecular dynamic simulation was used to study the functional impact of the three mutations E545K, E542K and L551Q on the protein structure. Our MD simulation studies revealed that the helical domain mutations prevent the allosteric regulation of p110α catalytic activity.

PIK3CA is one of the significantly mutated genes in breast cancer with ~40% frequency. The role of *PIK3CA* mutations in pathophysiology and drug resistance in breast cancer is not well known. Several studies (28, 29) have suggested that helical domain mutations are associated with resistance of HER2-positive breast cancer to trastuzumab. Here, we investigated the exon 9 of *PIK3CA* as a hotspot region to helical domain mutations. For the first time, we found a novel mutation in p110α, L551Q, which could be functionally carcinogenic.

The interaction between p110α helical domain with nSH2 domain of p85α is not yet fully uncovered. Therefore, we performed an MD analysis comparing DCCM and PC1 between WT and mutants. Our results showed that helical domain mutations extremely affect dynamics of p110α-p85α complex. In addition, communication network analysis displayed that the helical domain mutations disrupt the connection between helical and kinase domains. The defective allostery in each mutant affects p110α substrate binding pocket (SBP) differently, resulting in various SBP shapes in each mutant.

Previous MD simulation studies of p110α helical domain mutants have shown that E542K and E545K mutations disrupt nSH2 interactions with helical domain, which results in helical domain detachment (30). We also observed a similar partial detachment. It has been shown that p85α stabilizes p110α, and the enzyme needs its regulatory partner for better functionality (31). However, helical domain mutations result in a p110α enzymatic activity independent of p85α (10). Thus, the helical domain mutations result in a p110α which benefits from the stabilizing effects of p85α, but does not receive its inhibitory signals.

Gkeka and colleagues (32) have found that SBP is more compact in WT than in H1047R, suggesting WT has an intrinsic resistance to substrates binding. Here we found that SBP shape in the kinase domain is

different in WT compared to that of mutants, and even between mutants. The major difference in SBP shape is seen between E542K and E545K mutants. This may suggest that mutants of helical domain may have different substrate affinities. Notably, p110α inhibitors bind to this pocket and any structural changes in SBP could affect drug affinity for p110α (33). Thus, we suggest that genotyping *PIK3CA* in breast tumors prior to the treatment could have clinical implications, as we speculate that a specific p110α inhibitor could have different outcomes in each p110α mutant. Indeed, p110α has role in drug resistance in cancer patients (34). However, our simulations do not include anti-p110α effects on helical domain mutants, but it would be of great interest if anti-p110α drugs affinity be measured for all of the helical domain mutants.

Various functional studies on *PIK3CA* mutations have been carried out of which, Meyer *et al* have investigated the overexpression of E545K in a transgenic mouse model. Notably, E545K mutation induces heterogeneous mammary carcinomas but with longer latency than H1047R (35). Another study on E545K and E542K in chicken embryonic fibroblasts suggested that the gain of function induced by helical domain mutations is independent of binding to p85 but requires interaction with RAS-GPT (10). Another *in vivo* study on induced tumors in the chorioallantoic membrane of the chicken embryo showed that the three prevalent mutants of p110α, E542K, E545K, and H1047R are able to promote angiogenesis and increase the activation of the Akt pathway (36, 37).

A recent study by Vasan N *et al*. (38) showed that double *PIK3CA* mutations can result in increased activity of PI3K activity and downstream signaling pathways. Although we were not able to test whether E542K and L551Q are on the same allele, it is plausible that these two mutations may have synergistic effect on tumor growth. Future studies are warranted to investigate the function of double mutations in tumor cells proliferation and more importantly, response to PI3K inhibitors.

Conclusions

Our MD simulations show that L551Q mutation has a functional dynamics network similar to E542K and E545K mutations and thus, may have similar carcinogenic activity. However, we suggest that future *in vitro/vivo* studies are warranted to characterize the potential carcinogenic activity of L551Q mutation in breast cancer.

Declarations

Ethics approval and consent to participate:

This manuscript does not contain any study with animal performed and all of studies involving

All the patients were consented according to the ethical standards of the Isfahan University of Medical Sciences with reference number: ir.mui.rec.1396.3.131. Written consent was obtained from all the patients.

Consent for publication:

Written informed consent was signed by all the authors included in the study.

Availability of data and material:

The datasets used and/or analyzed during this study is available by the corresponding authors upon request.

Competing interests:

The authors declare that there is no conflict of interests.

Funding

This study was funded by medical university of Isfahan scholarship which provides analysis, collection, and interpretation of data.

Authors' Contributions

Designing the study and collection of data by SG, designing and analysis of the MD simulations by SA, writing the manuscript by SG, HM, SA, and AB, providing material and tumor samples by FK and HM, interpretation of the data by AB, final approval of study by MS and AB

Acknowledgments

The authors thank the patients for their participation in this study. In addition, they thank Dr.

Sayyed Mohammadreza Hakimian for providing tumors tissues.

References

1. Ferlay J, Héry C, Autier P, Sankaranarayanan R. Global burden of breast cancer. Breast cancer epidemiology: Springer; 2010. p. 1-19.
2. Siegel RL, Miller KD, Jemal A. Cancer statistics, 2018. CA: A Cancer Journal for Clinicians. 2018;68(1):7-30.
3. Mukohara T. PI3K mutations in breast cancer: prognostic and therapeutic implications. Breast Cancer: Targets and Therapy. 2015;7:111.
4. Luo J, Manning BD, Cantley LC. Targeting the PI3K-Akt pathway in human cancer. Cancer cell. 2003;4(4):257-62.
5. Amzel LM, Huang C-H, Mandelker D, Lengauer C, Gabelli SB, Vogelstein B. Structural comparisons of class I phosphoinositide 3-kinases. Nature Reviews Cancer. 2008;8(9):665.

6. Network CGA. Comprehensive molecular portraits of human breast tumours. Nature. 2012;490(7418):61-70.
7. Pereira B, Chin S-F, Rueda OM, Vollan H-KM, Provenzano E, Bardwell HA, et al. The somatic mutation profiles of 2,433 breast cancers refine their genomic and transcriptomic landscapes. Nature communications. 2016;7:11479.
8. Samuels Y, Wang Z, Bardelli A, Silliman N, Ptak J, Szabo S, et al. High frequency of mutations of the PIK3CA gene in human cancers. Science. 2004;304(5670):554-.
9. Miled N, Yan Y, Hon W-C, Perisic O, Zvelebil M, Inbar Y, et al. Mechanism of two classes of cancer mutations in the phosphoinositide 3-kinase catalytic subunit. science. 2007;317(5835):239-42.
10. Zhao L, Vogt PK. Helical domain and kinase domain mutations in p110α of phosphatidylinositol 3-kinase induce gain of function by different mechanisms. Proceedings of the National Academy of Sciences. 2008;105(7):2652-7.
11. Liu S, Knapp S, Ahmed AA. The structural basis of PI3K cancer mutations: from mechanism to therapy. Cancer research. 2014.
12. Huang C-H, Mandelker D, Schmidt-Kittler O, Samuels Y, Velculescu VE, Kinzler KW, et al. The structure of a human p110α/p85α complex elucidates the effects of oncogenic PI3Kα mutations. Science. 2007;318(5857):1744-8.
13. Ramensky V, Bork P, Sunyaev S. Human non-synonymous SNPs: server and survey. Nucleic acids research. 2002;30(17):3894-900.
14. Ng PC, Henikoff S. SIFT: Predicting amino acid changes that affect protein function. Nucleic acids research. 2003;31(13):3812-4.
15. Schwarz JM, Cooper DN, Schuelke M, Seelow D. MutationTaster2: mutation prediction for the deep-sequencing age. Nature methods. 2014;11(4):361.
16. Choi Y, Chan AP. PROVEAN web server: a tool to predict the functional effect of amino acid substitutions and indels. Bioinformatics. 2015;31(16):2745-7.
17. Capriotti E, Calabrese R, Casadio R. Predicting the insurgence of human genetic diseases associated to single point protein mutations with support vector machines and evolutionary information. Bioinformatics. 2006;22(22):2729-34.
18. Capriotti E, Fariselli P, Casadio R. I-Mutant2. 0: predicting stability changes upon mutation from the protein sequence or structure. Nucleic acids research. 2005;33(suppl_2):W306-W10.
19. Venselaar H, te Beek TA, Kuipers RK, Hekkelman ML, Vriend G. Protein structure analysis of mutations causing inheritable diseases. An e-Science approach with life scientist friendly interfaces. BMC bioinformatics. 2010;11(1):548.
20. Forbes SA, Beare D, Gunasekaran P, Leung K, Bindal N, Boutselakis H, et al. COSMIC: exploring the world's knowledge of somatic mutations in human cancer. Nucleic acids research. 2014;43(D1):D805-D11.
21. Micheel CM, Lovly CM, Levy MA. My cancer genome. Cancer Genetics. 2014;207(6):289.

22. Cerami E, Gao J, Dogrusoz U, Gross BE, Sumer SO, Aksoy BA, et al. The cBio cancer genomics portal: an open platform for exploring multidimensional cancer genomics data. AACR; 2012.
23. Miller MS, Schmidt-Kittler O, Bolduc DM, Brower ET, Chaves-Moreira D, Allaire M, et al. Structural basis of nSH2 regulation and lipid binding in PI3Kα. Oncotarget. 2014;5(14):5198.
24. D.A. Case RMB, D.S. Cerutti, T.E. Cheatham, III, T.A. Darden, R.E. Duke, T.J. Giese, H. Gohlke, A.W. Goetz, N. Homeyer, S. Izadi, P. Janowski, J. Kaus, A. Kovalenko, T.S. Lee, S. LeGrand, P. Li, C. Lin, T. Luchko, R. Luo, B. Madej, D. Mermelstein, K.M. Merz, G. Monard, H. Nguyen, H.T. Nguyen, I. Omelyan, A. Onufriev, D.R. Roe, A. Roitberg, C. Sagui, C.L. Simmerling, W.M. Botello-Smith, J. Swails, R.C. Walker, J. Wang, R.M. Wolf, X. Wu, L. Xiao and P.A. Kollman (2016). AMBER 2016. University of California, San Francisco.2016.
25. Grant BJ, Rodrigues AP, ElSawy KM, McCammon JA, Caves LS. Bio3d: an R package for the comparative analysis of protein structures. Bioinformatics. 2006;22(21):2695-6.
26. Vogt PK. Drug-resistant phosphatidylinositol 3-kinase: guidance for the preemptive strike. Cancer cell. 2008;14(2):107-8.
27. Zunder ER, Knight ZA, Houseman BT, Apsel B, Shokat KM. Discovery of drug-resistant and drug-sensitizing mutations in the oncogenic PI3K isoform p110 alpha. Cancer Cell. 2008;14(2):180-92.
28. Berns K, Horlings HM, Hennessy BT, Madiredjo M, Hijmans EM, Beelen K, et al. A functional genetic approach identifies the PI3K pathway as a major determinant of trastuzumab resistance in breast cancer. Cancer cell. 2007;12(4):395-402.
29. Nagata Y, Lan K-H, Zhou X, Tan M, Esteva FJ, Sahin AA, et al. PTEN activation contributes to tumor inhibition by trastuzumab, and loss of PTEN predicts trastuzumab resistance in patients. Cancer cell. 2004;6(2):117-27.
30. Leontiadou H, Galdadas I, Athanasiou C, Cournia Z. Insights into the mechanism of the PIK3CA E545K activating mutation using MD simulations. Scientific reports. 2018;8(1):15544.
31. Yu J, Zhang Y, McIlroy J, Rordorf-Nikolic T, Orr GA, Backer JM. Regulation of the p85/p110 phosphatidylinositol 3'-kinase: stabilization and inhibition of the p110α catalytic subunit by the p85 regulatory subunit. Molecular and cellular biology. 1998;18(3):1379-87.
32. Gkeka P, Evangelidis T, Pavlaki M, Lazani V, Christoforidis S, Agianian B, et al. Investigating the structure and dynamics of the PIK3CA wild-type and H1047R oncogenic mutant. PLoS computational biology. 2014;10(10):e1003895.
33. Zhao Y, Zhang X, Chen Y, Lu S, Peng Y, Wang X, et al. Crystal structures of PI3Kα complexed with PI103 and its derivatives: new directions for inhibitors design. ACS medicinal chemistry letters. 2013;5(2):138-42.
34. Falasca M. PI3K/Akt signalling pathway specific inhibitors: a novel strategy to sensitize cancer cells to anti-cancer drugs. Current pharmaceutical design. 2010;16(12):1410-6.
35. Meyer D, Koren S, Leroy C, Brinkhaus H, Müller U, Klebba I, et al. Expression of PIK3CA mutant E545K in the mammary gland induces heterogeneous tumors but is less potent than mutant H1047R. Oncogenesis. 2013;2(9):e74.

36. Ikenoue T, Kanai F, Hikiba Y, Obata T, Tanaka Y, Imamura J, et al. Functional analysis of PIK3CA gene mutations in human colorectal cancer. Cancer research. 2005;65(11):4562-7.
37. Bader AG, Kang S, Vogt PK. Cancer-specific mutations in PIK3CA are oncogenic in vivo. Proceedings of the National Academy of Sciences. 2006;103(5):1475-9.
38. Vasan N, Razavi P, Johnson JL, Shao H, Shah H, Antoine A, et al. Double PIK3CA mutations in cis increase oncogenicity and sensitivity to PI3Kalpha inhibitors. Science. 2019;366(6466):714-23.

Tables

Table 1. Clinical data in addition to PCR Sequencing results of patient samples diagnosed with mutations in *PIK3CA*

Patient no.	Age (years)	Breast cancer type	Grading/staging	ER/PR/HER2 status	Mutations detected by PCR sequencing
29	50-53	Invasive ductal carcinoma	T2N1MX	NA	E545K
45	39-42	Invasive ductal carcinoma	T2N3MX	ER+, PR+, HER2-	E542K, L551Q
24	40-45	Invasive lobular carcinoma	T2N0MX	ER+, HER2-	E542K
3	42-48	Invasive ductal carcinoma	NA	NA	NA

Table 2. Various sequencing software's for predicting variant.

	Variant	L551Q
MutationTaster	Score	113
	Prediction	Disease-causing
PolyPhen2	Score	1.000
	Prediction	Probably damaging
SIFT	Score	0.00
	Prediction	Damaging
PROVEAN	Prediction	Deleterious
	Score	-4.73
PhD-SNP	RI	5
	Prediction	Disease-related polymorphism
I-Mutant	DDG value Kcal/mol	-1.91
	SVM prediction	Decrease stability
	RI	8

PROVEAN prediction Cut of f = -2.5, **RI**: Reliability Index, **DDG**: DDG, **SVM**: support vector, **SVM2 value**: DDG < 0: decrease stability, DDG >0 increase stability

Figures

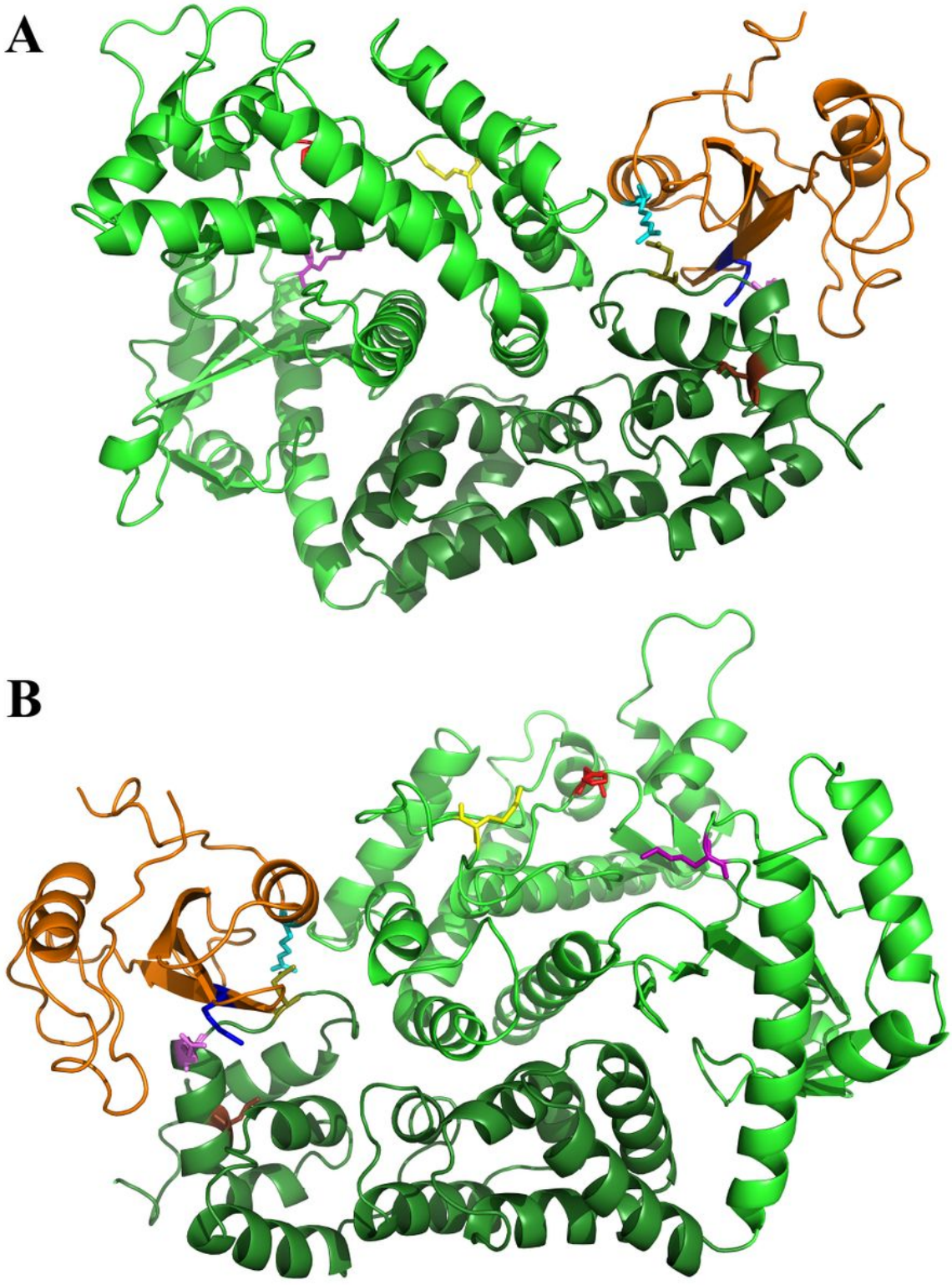

Figure 1

The central part of the p110α-p85α complex. A: Taken form PDB ID 4OVU, only p110α helical (dark green helices) and kinase (light green helices) domains and p85α nSH2 domain (orange moiety) are shown. Amino acids discussed in the text are showed in sticks and colored as follow: E542 (olive), E545 (pink),

and L551 (brown) in p110α helical domain, K776 (purple), H917 (red), and K941 (yellow) in p110α kinase domain, R340 (cyan), and K379 (blue) in p85α nSH2 domain. (all structural representations in later figures have the same orientation as this representation) B: The p110α-p85α complex rotated 180° around the vertical axis.

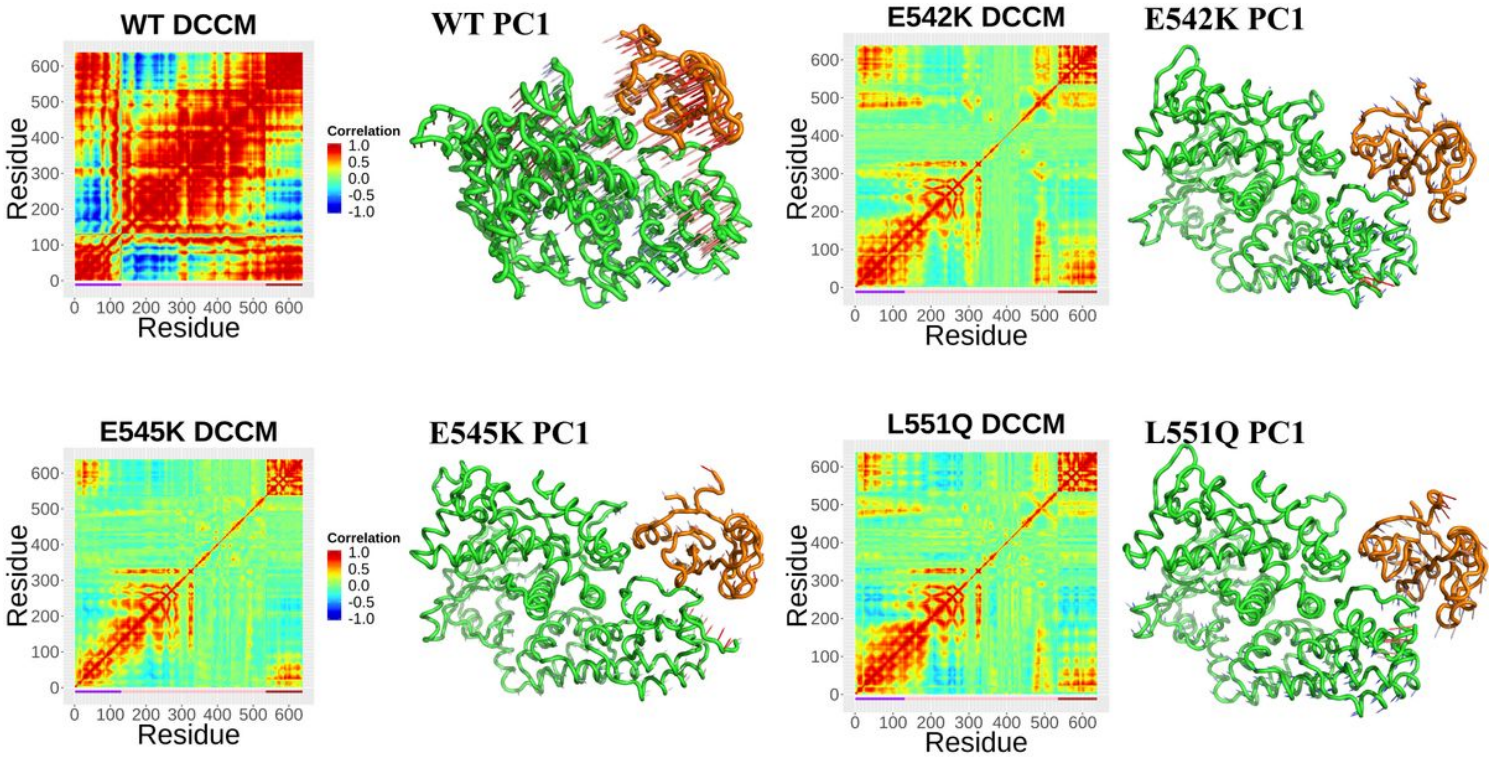

Figure 2

Motions and correlations in the p110α-p85α complex. WT and mutants DCCMs are shown as heatmaps and the simulation dynamics of each protein is displayed in PC1 graphs (green: p110α, orange: p85α, arrows indicate motions intensity). The color strip on the horizontal axis of the DCCMs defines the range of each domain in the complex sequence as follow: helical domain in purple, kinase domain in pink, and nSH2 domain in brown. All structural representations are as Figure 1A.

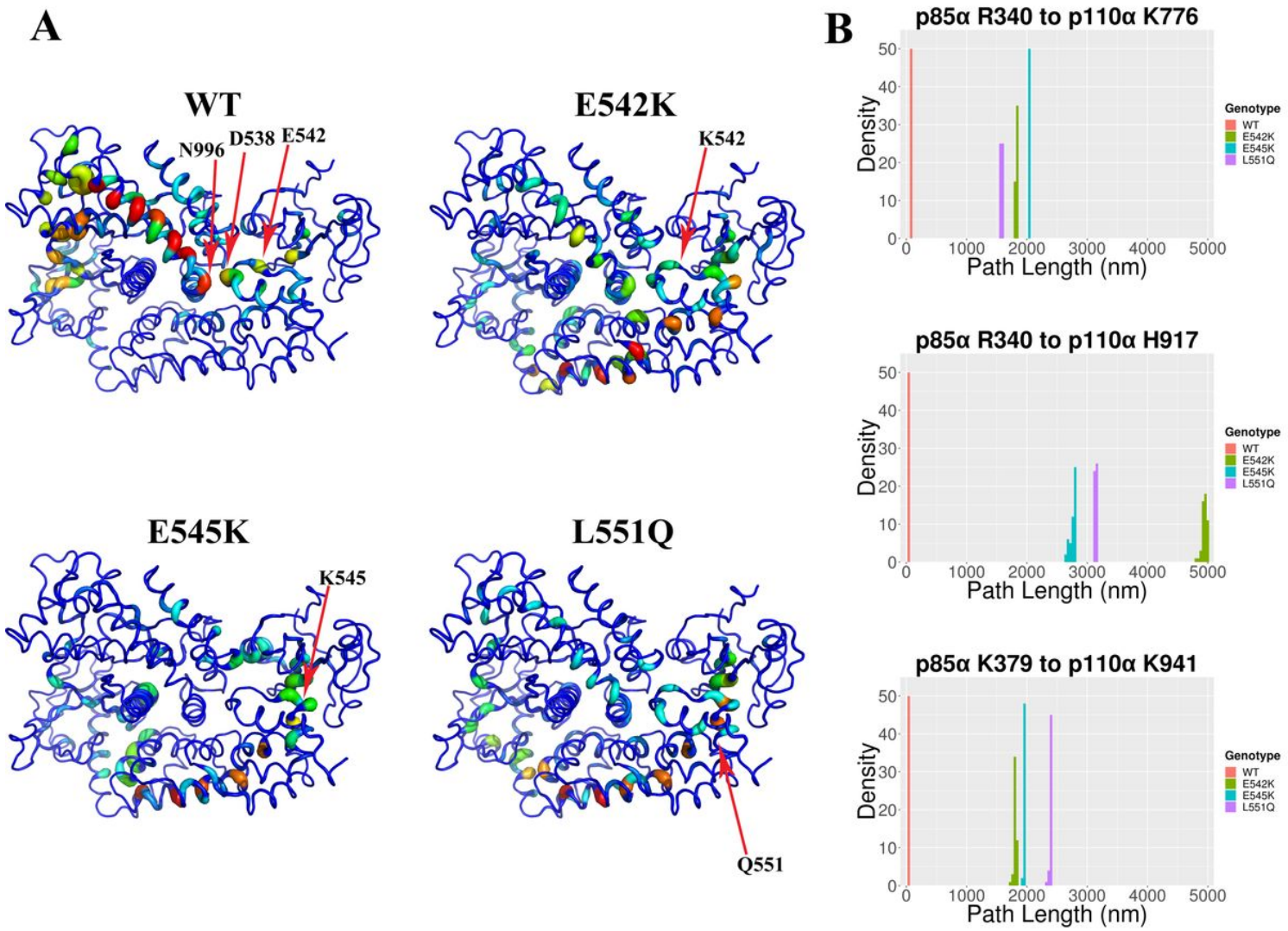

Figure 3

Communication network analysis. A: Centrality of the residues in dynamical behavior of p110α-p85α complex. The color spectrum shows the degree of centrality in dynamics coordination from dark blue (less central) to red (more central). Red arrows indicate the location of residues of interest (discussed in the text). Orientation of the structures are same as Figure 1A. B: The distance that an allosteric signal passes from start site to the end. Longer paths could weaken the signal.

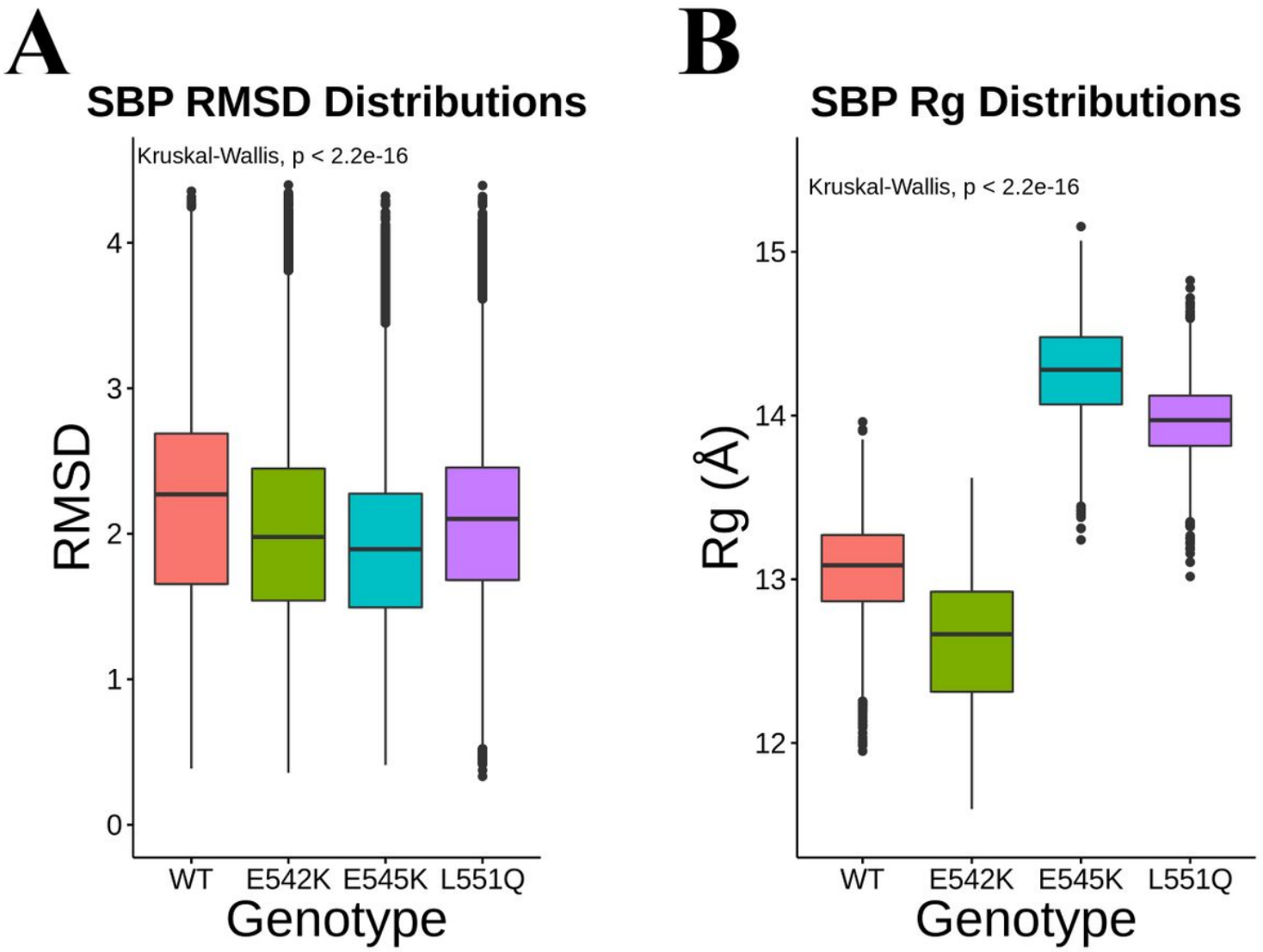

Figure 4

p110α substrate binding pocket flexibility and shape. A: SBP flexibility was measured by calculating distribution of pairwise RMSDs of each system. B: Distribution of SBP Rg among different mutants that could be an indication of SBP shape. Kruskal-Wallis test was used to test if the difference between the medians is significant.